Thermophoresis of an Aerosol Sphere Perpendicular to Two Plane Walls

Huan J. Keh and Yu C. Chang
Dept. of Chemical Engineering, National Taiwan University, Taipei 10617 Taiwan, ROC

DOI 10.1002/aic.10788
Published online February 15, 2006 in Wiley InterScience (www.interscience.wiley.com).

The problem of the thermophoretic motion of a spherical particle in a gaseous medium situated at an arbitrary position between two infinite parallel plane walls is studied theoretically in the quasisteady limit of negligible Peclet and Reynolds numbers. The imposed temperature gradient is uniform and perpendicular to the plane walls. The Knudsen number is assumed to be small so that the fluid flow is described by a continuum model with a temperature jump, a thermal slip, and a frictional slip at the particle surface. The presence of the confining walls causes two basic effects on the particle velocity: first, the local temperature gradient on the particle surface is altered by the walls, thereby speeding up or slowing down the particle; second, the walls enhance the viscous retardation of the moving particle. A boundary collocation method is used to solve the thermal and hydrodynamic governing equations of the system. Numerical results for the thermophoretic velocity of the particle relative to that under identical conditions in an unbounded gaseous medium are presented for various cases. The collocation results agree well with the available approximate analytical solutions obtained by using a method of reflections. The presence of the walls can reduce or enhance the particle velocity, depending upon the relative thermal conductivity and surface properties of the particle as well as the relative particle-wall separation distances. The boundary effect on thermophoresis of a particle normal to two plane walls is found to be quite significant and generally stronger than that parallel to the confining walls. © 2006 American Institute of Chemical Engineers *AIChE J,* 52: 1690–1704, 2006

Keywords: thermophoresis, aerosol sphere, continuum regime, fluid mechanics, boundary effect, plane walls

Introduction

A particle, when suspended in a gas possessing a temperature gradient, acquires a velocity relative to the gas in the direction of decreasing temperature. This phenomenon, known as thermophoresis, was first observed by Tyndall in 1870 when it was discovered that a dust-free space surrounded a hot body.[1] The thermophoretic effect can be explained in part by appealing to the kinetic theory of gases.[2] The higher energy molecules in the hot regions of the gas impinge on the particle with greater momenta than molecules coming from the cold regions, thus resulting in the migration of the particle in the direction of decreasing temperature. Being a mechanism for the capture of aerosol particles on cool surfaces, thermophoresis is of considerable importance in many practical applications, such as sampling of aerosol particles,[3] cleaning of air,[4] scale formation on surfaces of heat exchangers,[5] modified chemical vapor deposition,[6] manufacturing of microelectronics,[7] nuclear reactor safety,[8] and removal of soot aerosol particles for combustion exhaust gas systems.[9,10]

On the basis of the assumptions of small Knudsen number (l/a, where a is the radius of the particle and l is the mean free path of the gas molecules), small Peclet number, and small Reynolds number, as well as the effects of temperature jump,

Correspondence concerning this article should be addressed to H. J. Keh at huan@ntu.edu.tw.

thermal slip, and frictional slip at the particle surface, the thermophoretic velocity of an aerosol sphere in a constant temperature gradient ∇T_∞ has been obtained as[11-14]

$$\mathbf{U}_0 = -A\nabla T_\infty, \tag{1}$$

where the thermophoretic mobility

$$A = \left[\frac{2C_s(k + k_1C_t l/a)}{(1 + 2C_m l/a)(2k + k_1 + 2k_1C_t l/a)}\right]\frac{\eta_f}{\rho_f T_0}. \tag{2}$$

In Eq. 2, ρ_f, η_f, and k are the density, viscosity, and thermal conductivity, respectively, of the gas; k_1 is the thermal conductivity of the particle; T_0 is the bulk-gas absolute temperature at the particle center in the absence of the particle (or the mean gas temperature in the vicinity of the particle); and C_s, C_t, and C_m are dimensionless coefficients accounting for the thermal slip, temperature jump, and frictional slip phenomena, respectively, at the particle surface and must be determined experimentally for each gas-solid system.

Satisfactory agreement of the prediction by Eq. 2 with experiments[15,16] has been obtained. Derjaguin et al.[17,18] presented the experimental data of the thermophoretic mobility for a variety of aerosols, which are in good agreement with Eq. 2 with $C_m = 0$, $C_s = 3/2$, and a suitable selection of the coefficient C_t. A set of kinetic-theory values for complete thermal and momentum accommodations appear to be $C_s = 1.17$, $C_t = 2.18$, and $C_m = 1.14$.[12] Recently, kinetic-theory values of these slip coefficients have been obtained accurately under various conditions.[19,20] Note that the negative sign in Eq. 1 indicates that the particle migration is in the direction opposite to the temperature gradient and $\rho_f T_0$ in Eq. 2 is a constant for an ideal gas at constant pressure. According to these equations, particles with large thermal conductivity and small Knudsen number (say, $k_1/k = 100$ and $l/a = 0.01$) will migrate by thermophoresis at velocities of 10-50 μm/s in temperature gradients of order 100 K/cm; such gradients are easily attainable in thermal boundary layers.

In most real situations of thermophoresis, aerosol particles are not isolated and the surrounding fluid is externally bounded by solid walls. Through an exact representation in spherical bipolar coordinates, the quasisteady thermophoretic motion of an aerosol sphere normal to a plane wall was semianalytically examined.[21] Numerical results of correction to Eq. 2 for the particle mobility were presented for various cases. Later, approximate analytical solutions for the thermophoretic mobility of a sphere near a plane wall in asymptotic forms were obtained using a method of reflections.[22] The thermophoresis of an aerosol sphere in a spherical cavity[23,24] and in a cylindrical pore[25] were also theoretically studied. Recently, the thermophoretic motion of an aerosol sphere parallel to two plane walls at an arbitrary position between them has been investigated by Keh and Chen[26] using both a boundary collocation technique and the method of reflections. Exact numerical results and approximate analytical solutions of the wall-correction to Eq. 2 for the particle mobility were presented for various values of the relative separation distances and other relevant parameters.

This article is an extension of the previous work[26] to the situation of the thermophoretic motion of a spherical particle perpendicular to two parallel plane walls at an arbitrary position between them. The effects of fluid inertia as well as thermal convection are neglected. For the case of a particle with a relatively high thermal conductivity undergoing thermophoresis normal to the plane walls, the heat conduction around the particle may generate larger temperature gradients on the particle surface relative to those in an infinite medium. These gradients enhance the thermophoretic velocity, although their action will be retarded by the viscous interaction of the migrating particle with the walls. Both effects of this thermal enhancement and the hydrodynamic retardation increase as the ratios of the radius of the particle to its distances from the walls increase. Determining which effect is overriding at small particle-wall gap widths is a main target of this study. Because the governing equations and boundary conditions concerning the general problem of thermophoresis of a particle at an arbitrary position between two parallel plane walls in an arbitrary direction are linear, its solution can be obtained as a superposition of the solutions for its two subproblems: motion parallel to the plane walls, which was previously examined,[26] and motion normal to the confining walls, which is considered in this article.

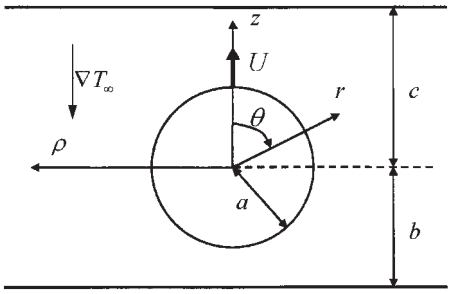

Figure 1. Geometrical sketch for the thermophoresis of a spherical particle perpendicular to two plane walls at an arbitrary position between them.

Analysis

We consider the quasisteady thermophoresis of a rigid spherical particle of radius a in a gaseous medium perpendicular to two infinite plane walls whose distances from the center of the particle are b and c, as shown in Figure 1. Here (ρ, ϕ, z) and (r, θ, ϕ) denote the circular cylindrical and spherical coordinate systems, respectively, and the origin of coordinates is chosen at the particle center. A linear temperature field $T_\infty(z)$ with a uniform thermal gradient $-E_\infty \mathbf{e}_z$ ($= \nabla T_\infty$) is imposed in the ambient fluid far removed from the particle, where $\mathbf{e}_z$ is the unit vector in the z direction and, for convenience, E_∞ is taken to be positive. It is assumed that the Knudsen number l/a is small so that the fluid flow is in the continuum regime and the Knudsen layer at the particle surface is thin in comparison with the radius of the particle and the spacing between the particle and each wall. The purpose is to obtain the correction to Eq. 2 for the particle mobility due to the presence of the plane walls.

To determine the thermophoretic velocity of the particle, it is necessary to ascertain the temperature distributions inside and outside the particle and the velocity field in the fluid phase.

Temperature distribution

For the heat transfer in a system of thermophoresis, the Peclet number can be assumed to be small. Hence, the energy equations governing the temperature distributions are

$$\nabla^2 T = 0 \quad (r \geq a) \tag{3a}$$

for the fluid and

$$\nabla^2 T_1 = 0 \quad (r \leq a) \tag{3b}$$

for the particle.

The boundary conditions at the particle surface require that the normal component of heat flux be continuous and that a temperature jump that is proportional to the normal temperature gradient[2] occur, namely,

$$r = a: \quad k \frac{\partial T}{\partial r} = k_1 \frac{\partial T_1}{\partial r}, \tag{4a}$$

$$T - T_1 = C_t l \frac{\partial T}{\partial r}. \tag{4b}$$

Here k and k_1 are the thermal conductivities of the fluid and particle, respectively, and C_t is the temperature jump coefficient about the surface of the particle; all are assumed to be constant. At the temperature range of 300-400 K, $k_1 = 0.022 - 0.024$ W $\cdot$ m^{-1} $\cdot$ K^{-1} for silica aerosol and $k_1 = 0.9 - 3$ W $\cdot$ m^{-1} $\cdot$ K^{-1} for clay, soil, and stone, while $k = 0.026 - 0.033$ W $\cdot$ m^{-1} $\cdot$ K^{-1} for air.[27] The dimensionless coefficient C_t is semi-empirically related to the thermal accommodation coefficient f_t [$= (E_i - E_r)/(E_i - E_w)$] at the particle-fluid interface by $C_t \cong (15/8)(2 - f_t)/f_t$, where E_i is the average incident energy flux at a point on the surface, E_r is the average reflected energy flux at that point, and E_w is that energy flux that would be emitted if the molecules left in thermal equilibrium with the surface at that point.[1]

Since the temperature far away from the particle approaches the undisturbed distribution, we can write

$$z = c: \quad T = T_0 - E_\infty c, \tag{5}$$

$$z = -b: \quad T = T_0 + E_\infty b, \tag{6}$$

$$\rho \to \infty: \quad T \to T_\infty = T_0 - E_\infty z. \tag{7}$$

The temperatures at the two parallel plane walls have been set equal to different constants to allow a uniform thermal gradient in their normal direction far from the particle.

The external temperature distribution, which is governed by the linear Laplace equation, can be expressed as the superposition

$$T = T_0 - E_\infty z + T_w + T_p. \tag{8}$$

Here, T_w is a separable solution of Eq. 3a in cylindrical coordinates that represents the disturbance produced by the plane walls and is given by a Fourier-Bessel integral

$$T_w = E_\infty \int_0^\infty [X(\omega) e^{\omega z} + Y(\omega) e^{-\omega z}] \omega J_0(\omega \rho) \mathrm{d}\omega, \tag{9}$$

where J_n is the Bessel function of the first kind of order n, and $X(\omega)$ and $Y(\omega)$ are unknown functions of the separation variable ω. The last term on the right-hand side of Eq. 8, T_p, is a separable solution of Eq. 3a in spherical coordinates representing the disturbance generated by the particle and is given by an infinite series in harmonics,

$$T_p = E_\infty \sum_{m=0}^{\infty} R_m r^{-m-1} P_m(\cos\theta), \tag{10}$$

where P_m is the Legendre polynomial of order m and R_m is an unknown constant. Note that a solution for T of the form given by Eqs. 8-10 immediately satisfies the boundary condition at infinity in Eq. 7. Since the temperature is finite for any position in the interior of the particle, the solution to Eq. 3b can be written as

$$T_1 = T_0 + E_\infty \sum_{m=0}^{\infty} \bar{R}_m r^m P_m(\cos\theta), \tag{11}$$

where $\bar{R}_m$ is an unknown constant.

Substituting the temperature distribution T given by Eqs. 8-10 into the boundary conditions in Eqs. 5 and 6 and applying the Hankel transform on the variable ρ leads to a solution for the functions $X(\omega)$ and $Y(\omega)$ in terms of the coefficients R_m. After the substitution of this solution into Eqs. 8-10, T can be expressed as

$$T = T_0 - E_\infty z + E_\infty \sum_{m=0}^{\infty} R_m \delta_m^{(1)}(r, \theta), \tag{12}$$

where the function $\delta_m^{(1)}(r, \theta)$ is defined by Eq. B1 in the Appendix (in which the integration must be performed numerically). Applying the boundary conditions given by Eq. 4 to Eqs. 11 and 12 yields

$$\sum_{m=0}^{\infty} [R_m \delta_m^{(2)}(a, \theta) - \bar{R}_m k^* m a^{m-1} P_m(\cos\theta)] = \cos\theta, \tag{13a}$$

$$\sum_{m=0}^{\infty} \{R_m [\delta_m^{(1)}(a, \theta) - a C_t^* \delta_m^{(2)}(a, \theta)] - \bar{R}_m a^m P_m(\cos\theta)\} = a(1 - C_t^*)\cos\theta, \tag{13b}$$

where $k^* = k_1/k$, $C_t^* = C_t l/a$, and the definition of the function $\delta_m^{(2)}(r, \theta)$ [$= \partial \delta_m^{(1)}/\partial r$] is given by Eq. B2.

To satisfy the conditions in Eq. 13 exactly along the entire surface of the particle would require the solution of the entire infinite array of unknown constants R_m and $\bar{R}_m$. However, the collocation method[26,28,29] enforces the boundary conditions at a finite number of discrete points on any semi-circular longitudinal generating arc of the sphere (from $\theta = 0$ to $\theta = \pi$) and truncates the infinite series in Eqs. 11 and 12 into finite ones. If the spherical boundary is approximated by satisfying the conditions of Eq. 4 at M discrete points on the generating arc, the infinite series in Eqs. 11 and 12 are truncated after M terms, resulting in a system of $2M$ simultaneous linear algebraic equations in the truncated form of Eq. 13. This matrix equation can be numerically solved to yield the $2M$ unknown constants R_m and $\bar{R}_m$ required in the truncated form of Eqs. 11 and 12 for the temperature distributions. The accuracy of the boundary-collocation/truncation technique can be improved to any degree by taking a sufficiently large value of M. Naturally, as $M \to \infty$ the truncation error vanishes and the overall accuracy of the solution depends only on the numerical integration required in evaluating the functions $\delta_m^{(1)}$ and $\delta_m^{(2)}$ in Eq. 13.

Fluid velocity distribution

Having obtained the solution for the external temperature distribution on the particle surface that drives the thermophoretic migration, we can now proceed to find the flow field. Owing to the low Reynolds number encountered in thermophoresis, the fluid motion is governed by the quasisteady fourth-order differential equation for viscous axisymmetric creeping flows,

$$E^2(E^2\Psi) = 0, \tag{14}$$

in which the Stokes stream function Ψ is related to the components of fluid velocity $\mathbf{v}$ in cylindrical coordinates by ($\nu_\phi = 0$)

$$v_\rho = \frac{1}{\rho}\frac{\partial \Psi}{\partial z}, \tag{15a}$$

$$v_z = -\frac{1}{\rho}\frac{\partial \Psi}{\partial \rho}, \tag{15b}$$

and the Stokes operator E^2 has the form

$$E^2 = \rho \frac{\partial}{\partial \rho}\left(\frac{1}{\rho}\frac{\partial}{\partial \rho}\right) + \frac{\partial^2}{\partial z^2}. \tag{16}$$

The boundary conditions for the fluid velocity at the particle surface,[11] on the plane walls, and far from the particle are

$$r = a: \quad \mathbf{v} = U\mathbf{e}_z + \frac{C_m l}{\eta_f}\tau_{r\theta}\mathbf{e}_\theta + \frac{C_s \eta_f}{\rho_f T_0}\frac{\partial T}{r\partial \theta}\mathbf{e}_\theta, \tag{17}$$

$$z = c, -b: \quad \mathbf{v} = \mathbf{0}, \tag{18}$$

$$\rho \to \infty: \quad \mathbf{v} = \mathbf{0}, \tag{19}$$

where $\tau_{r\theta}$ is the shear stress for the fluid, $\mathbf{e}_\theta$ is the unit vector in the θ direction, and U is the thermophoretic velocity of the particle to be determined. Note that, for the simplicity of mathematical analysis, we have neglected the possible frictional slip at the isothermal plane walls in the vicinity of the axis of symmetry, and this compromise is justified by the relevant results of previous analyses.[21,30]

To solve the flow field, we express the stream function in the form[29]

$$\Psi = \Psi_w + \Psi_p. \tag{20}$$

Here Ψ_w is a Fourier-Bessel integral solution of Eq. 14 in cylindrical coordinates that represents the disturbance produced by the plane walls and is given by

$$\Psi_w = \int_0^\infty [A(\omega)e^{\omega z} + B(\omega)e^{-\omega z} + C(\omega)\omega z e^{\omega z} + D(\omega)\omega z e^{-\omega z}]\rho J_1(\omega\rho)\mathrm{d}\omega, \tag{21}$$

where $A(\omega)$, $B(\omega)$, $C(\omega)$, and $D(\omega)$ are unknown functions of ω. The second part of Ψ, denoted by Ψ_p, is a separable solution of Eq. 14 in spherical coordinates representing the disturbance generated by the aerosol sphere and is given by

$$\Psi_p = \sum_{n=2}^{\infty} (B_n r^{-n+1} + D_n r^{-n+3})G_n^{-1/2}(\cos\theta), \tag{22}$$

where $G_n^{-1/2}$ is the Gegenbauer polynomial of the first kind of order n and degree –1/2; B_n and D_n are unknown constants. Note that the boundary condition in Eq. 19 is immediately satisfied by a solution of the form given by Eqs. 20-22.

Substituting the stream function Ψ given by Eqs. 20-22 into the boundary conditions in Eq. 18 and applying the Hankel transform on the variable ρ lead to a solution for $A(\omega)$, $B(\omega)$, $C(\omega)$, and $D(\omega)$ in terms of the coefficients B_n and D_n. After the substitution of this solution into Eqs. 20-22, the fluid velocity components can be expressed as

$$v_\rho = \sum_{n=2}^{\infty} [B_n \gamma_{1n}^{(1)}(r, \theta) + D_n \gamma_{2n}^{(1)}(r, \theta)], \tag{23a}$$

$$v_z = \sum_{n=2}^{\infty} [B_n \gamma_{1n}^{(2)}(r, \theta) + D_n \gamma_{2n}^{(2)}(r, \theta)], \tag{23b}$$

where the definitions of the functions $\gamma_{in}^{(j)}$ for i and j equal to 1 or 2 are given by Eqs. B4 and B5 (in which the integration must be performed numerically).

The only boundary condition that remains to be satisfied is that on the particle surface. Substituting Eqs. 12 and 23 into Eq. 17, one obtains

$$\sum_{n=2}^{\infty} \{B_n[\gamma_{1n}^{(1)}(a,\theta) - C_m^* a\gamma_{1n}^*(a,\theta)\cos\theta] + D_n[\gamma_{2n}^{(1)}(a,\theta) - C_m^* a\gamma_{2n}^*(a,\theta)\cos\theta]\} = C_s \frac{\eta_f E_\infty}{\rho_f T_0} \times \left[\sin\theta + \sum_{m=0}^{\infty} R_m \delta_m^{(3)}(a,\theta)\right]\cos\theta, \quad (24a)$$

$$\sum_{n=2}^{\infty} \{B_n[\gamma_{1n}^{(2)}(a,\theta) + C_m^* a\gamma_{1n}^*(a,\theta)\sin\theta] + D_n[\gamma_{2n}^{(2)}(a,\theta) + C_m^* a\gamma_{2n}^*(a,\theta)\sin\theta]\} = U - C_s \frac{\eta_f E_\infty}{\rho_f T_0} \times \left[\sin\theta + \sum_{m=0}^{\infty} R_m \delta_m^{(3)}(a,\theta)\right]\sin\theta, \quad (24b)$$

where $C_m^* = C_m l/a$, the definition of the function $\delta_m^{(3)}(r,\theta)$ $[= \partial\delta_m^{(1)}/r\partial\theta]$ is given by Eq. B3, and the functions $\gamma_{in}^*(r,\theta)$ for i equal to 1 or 2 are defined by Eq. B14. The first M coefficients R_m have been determined through the procedure given in the previous subsection.

Equation 24 can be satisfied by utilizing the collocation technique presented for the solution of the temperature field. Along a longitudinal generating arc at the particle surface, Eq. 24 is applied at N discrete points (values of θ between 0 and π) and the infinite series in Eq. 23 are truncated after N terms. This generates a set of $2N$ linear algebraic equations for the $2N$ unknown coefficients B_n and D_n. The fluid velocity field is completely obtained once these coefficients are solved for a sufficiently large number of N.

Derivation of the particle velocity

The hydrodynamic force acting on the spherical particle can be determined from[31]

$$F = 4\pi\eta_f D_2, \quad (25)$$

where η_f is the fluid viscosity. This expression shows that only the lowest-order coefficient D_2 contributes to the drag force exerted on the particle by the fluid.

Since the particle is freely suspended in the surrounding fluid, the net force acting on the particle must vanish. Applying this constraint to Eq. 25, one has

$$D_2 = 0. \quad (26)$$

To determine the thermophoretic velocity U of the particle, Eq. 26 and the $2N$ algebraic equations resulting from Eq. 24 are to be solved simultaneously. Note that, similar to the thermophoretic velocity of an isolated sphere given by Eqs. 1 and 2, the value of U is proportional to the quantity $C_s\eta_f E_\infty/\rho_f T_0$ and dependent on the dimensionless parameters k^*, C_t^*, and C_m^* (in addition to the length ratios among a, b, and c).

If the particle velocity in Eq. 17 is disabled (i.e., $U = 0$ is set), then the force obtained from Eq. 25 can be taken as the thermophoretic force exerted on the particle near the walls due to the temperature gradient ∇T_∞. This force can be expressed as

$$F = 6\pi\eta_f a U_0 \frac{1 + 2C_m^*}{1 + 3C_m^*} F^*, \quad (27)$$

where U_0 is a characteristic velocity (the thermophoretic velocity of the particle in the absence of the plane walls) given by Eqs. 1 and 2 and F^* is the normalized magnitude of the thermophoretic force. The value of F^* also equals f^*U/U_0, where f^* is the dimensionless Stokes resistance coefficient of the slip particle migrating normal to the two plane walls driven by a body force in the absence of the temperature gradient[32] and U is the thermophoretic velocity of the particle obtained from Eq. 26.

Results and Discussion

The numerical results for the thermophoretic motion of a spherical particle perpendicular to two plane walls at an arbitrary position between them, obtained by using the boundary collocation method described in the previous section, is presented in this section. The system of linear algebraic equations to be solved for the coefficients R_m and $\bar{R}_m$ is constructed from Eq. 13, while that for B_n and D_n is composed of Eq. 24. All the numerical integrations to evaluate the functions $\delta_m^{(j)}$, $\gamma_{in}^{(j)}$, and γ_{in}^* were done by the 180-point Gauss-Laguerre quadrature.

When selecting the points along the half-circular generating arc of the spherical particle where the boundary conditions are to be exactly satisfied, the first points that should be chosen are $\theta = 0$ and $\theta = \pi$, since these stagnation points control the gaps between the particle and the plane walls. In addition, the point $\theta = \pi/2$, which defines the projected area of the particle normal to the direction of migration, is also important. However, an examination of the systems of linear algebraic Eqs. 13 and 24 shows that the matrix equations become singular if these points are used. To overcome this difficulty, these three points are replaced by four closely adjacent basic points, i.e., $\theta = \delta$, $\pi/2 - \delta$, $\pi/2 + \delta$, and $\pi - \delta$.[29] Additional points along the generating arc are selected as mirror-image pairs about the plane $\theta = \pi/2$ to divide the two quarter-circular arcs of the particle into equal segments. The optimum value of δ in this work is found to be 0.01°, with which the numerical results of the particle velocity converge satisfactorily.

In our continuum-with-slippage analysis given in the previous section, the Knudsen number (l/a) of the system should be smaller than about 0.1. As mentioned in the first section, a set of well adapted values for the temperature jump and frictional slip coefficients under the condition of complete energy and momentum accommodations are 2.18 and 1.14, respectively. Consequently, the normalized coefficients C_t^* and C_m^* must be restricted to be less than unity. For convenience, we will use the ratio $C_t^*/C_m^* = 2$ (a rounded value to 2.18/1.14 = 1.91) throughout this section, without the loss of reality or generality. On the other hand, the thermal conductivity of an aerosol particle is usually greater than that of the ambient gas. Thus, the value of the relative conductivity k^* will exceed unity under most practical situations.

Table 1. Normalized Thermophoretic Velocity of a Spherical Particle Perpendicular to a Single Plane Wall Computed from the Exact Boundary-Collocation Solution and the Asymptotic Method-of-Reflection Solution

	U/U_0			
	$C_t^* = 2C_m^* = 0$		$C_t^* = 2C_m^* = 0.02$	
a/b	Exact Solution	Asymptotic Solution	Exact Solution	Asymptotic Solution
		$k^* = 0$		
0.2	0.99504	0.99504	0.99504	0.99504
0.4	0.96020	0.96022	0.96022	0.96024
0.6	0.85862	0.86086	0.85913	0.86114
0.8	0.61631	0.65379	0.62079	0.65474
0.9	0.38584	0.50278	0.39821	0.50361
0.95	0.21993	0.41843	0.24005	0.41870
0.99	0.04960	0.34927	0.07243	0.34864
0.995	0.02522		0.04400	
0.999	0.00513		0.01323	
		$k^* = 10$		
0.2	0.99756	0.99756	0.99748	0.99748
0.4	0.98116	0.98115	0.98058	0.98056
0.6	0.93726	0.93806	0.93604	0.93641
0.8	0.84398	0.86067	0.84659	0.85736
0.9	0.76067	0.81623	0.77318	0.81099
0.95	0.69576	0.79775	0.71327	0.79073
0.99	0.56758	0.78755	0.51996	0.77842
0.995	0.49929		0.40467	
0.999	0.30723		0.16567	
		$k^* = 100$		
0.2	0.99800	0.99800	0.99790	0.99790
0.4	0.98489	0.98488	0.98457	0.98447
0.6	0.95175	0.95218	0.95650	0.95412
0.8	0.89311	0.90139	0.95155	0.91650
0.9	0.86725	0.88184	1.05829	0.90968
0.95	0.88977	0.88024	1.26159	0.91547
0.99	1.13484	0.88622	1.54030	0.92731
0.995	1.31468		1.37615	
0.999	1.82653		0.66626	

Motion normal to a single plane wall

Numerical solutions for the thermophoretic velocity of a spherical particle with $C_t^* = 2C_m^* = 0$ and 0.02 near a single plane wall (i.e., with $c \to \infty$) caused by a normal temperature gradient are presented in Table 1 for various values of the parameters k^* and a/b at the quasisteady state using the boundary collocation method. The velocity for the thermophoretic motion of an identical particle in an infinite fluid, $U_0 = -AE_\infty$, given by Eqs. 1 and 2, is used to normalize the boundary-corrected quantities. Thus, the normalized particle velocity is independent of the values of C_S, E_∞, η_f, and $\rho_f T_0$. The limiting case of $k^* = 0$, which is not likely to exist in practice, is considered here for the sake of numerical comparison. All of the results obtained under the collocation scheme converge satisfactorily to at least the significant figures shown in the table. The accuracy and convergence behavior of the truncation technique is principally a function of the ratio a/b. For general cases with $a/b \le 0.9$, the numbers $M = 26$ and $N = 26$ can lead to these satisfactory results. For the most difficult case with a/b, the numbers $M = 200$ and $N = 200$ are sufficiently large to achieve this convergence. Our collocation results can be found to agree excellently with the numerical solutions obtained by Chen and Keh[21] using spherical bipolar coordinates.

Using a method of reflections, Chen[22] obtained a power series expression in λ ($= a/b$) for the velocity of an aerosol sphere undergoing the same thermophoretic motion as that considered here. After correcting an error in the $O(\lambda^8)$ term of this expression, it becomes

$$U = U_0\left\{1 - \frac{1}{4}(2+G)\lambda^3 + \frac{1}{4}D\lambda^5 - \frac{1}{256} \times \left[27\left(5C + 4G\frac{B}{A}\right) - 16(2+G)G\right]\lambda^6 + \frac{1}{512} \times \left[27\left(5C + 4G\frac{B}{A}\right)D + 4(9H - 8D)G\right]\lambda^8 + O(\lambda^9)\right\}, \tag{28}$$

where

$$C = \frac{1 + 2C_m^*}{1 + 5C_m^*}, \tag{29a}$$

$$D = \frac{1}{1 + 2C_m^*}, \tag{29b}$$

$$G = \frac{1 - k^* + k^* C_t^*}{2 + k^* + 2k^* C_t^*}, \tag{29c}$$

$$H = \frac{1 - k^* + 2k^* C_t^*}{3 + 2k^* + 6k^* C_t^*}, \tag{29d}$$

$$B = \left[\frac{5C_s(1 + 2k^* C_t^*)}{2(1 + 5C_m^*)(3 + 2k^* + 6k^* C_t^*)}\right]\frac{\eta_f}{\rho_f T_0}, \tag{29e}$$

and A is defined by Eq. 2. The values of the wall-corrected normalized thermophoretic mobility calculated from this asymptotic solution, with the $O(\lambda^9)$ term neglected, are also listed in Table 1 for comparison. It can be seen that the asymptotic formula of Eq. 28 from the method of reflections for U/U_0 agrees very well with the exact results as long as $\lambda \le 0.6$; the errors in all cases are less than 0.3%. However, accuracy of Eq. 28 begins to deteriorate, as expected, when the relative spacing between the particle and the plane wall becomes small (say, $\lambda \ge 0.8$). The formula of Eq. 28 can overestimate or underestimate the thermophoretic velocity of the particle depending on relevant parameters.

The collocation solutions for the normalized velocity U/U_0 of a spherical particle with $C_t^* = 2C_m^* = 0.02$ and 0.2 undergoing thermophoresis normal to a plane wall as functions of a/b are depicted in Figure 2 for various values of k^*. As expected, the particle migrates with the velocity that would exist in the absence of the wall as $a/b \to 0$. However, the boundary effect of the plane wall on thermophoretic motion can be quite significant when a/b becomes greater. The wall-corrected normalized thermophoretic mobility U/U_0 of the particle increases with an increase in k^*, keeping the other parameters (C_t^*, C_m^*, and a/b) unchanged. This increase in the particle mobility in general becomes more pronounced as a/b increases (but is not too close to unity). This behavior is expected knowing that the local temperature gradients along the particle surface near an iso-

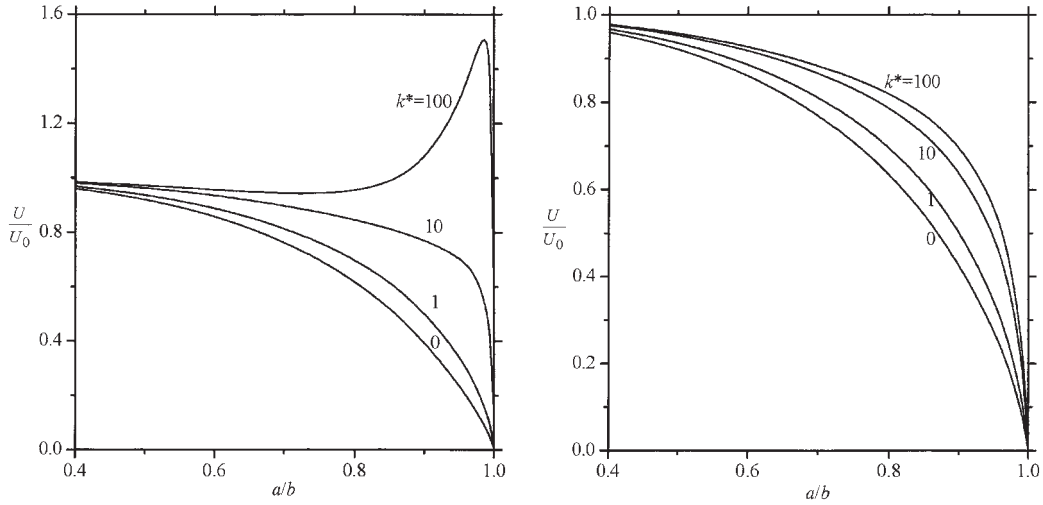

Figure 2. Plots of the normalized thermophoretic velocity U/U_0 of a spherical particle perpendicular to a plane wall vs. the separation parameter a/b for various values of k^*.

(a) With $C_t^* = 2C_m^* = 0.02$; (b) with $C_t^* = 2C_m^* = 0.2$.

thermal wall with a perpendicularly-imposed thermal gradient decrease as k^* decreases (the local temperature gradient at the particle surface on the near side to the plane wall is depressed compared with that on the far side, as can be seen in the analysis given in the Appendix or Keh and Lien[33]). When $k^* = (1 - C_t^*)^{-1}$, the effect of thermal interaction between the particle and the wall disappears, and the relative thermophoretic mobility of the particle decreases monotonically with a/b solely owing to the hydrodynamic resistance exerted by the plane wall.

Examination of the results shown in Table 1 and Figure 2a reveals an interesting feature when the particle has small values of C_t^* and C_m^*. For the case of large k^* (e.g., with $k^* = 100$), the thermophoretic mobility of the particle in the direction normal to a plane wall decreases with an increase in a/b as a/b is small, but increases from a minimum with increasing a/b as a/b is sufficiently large. When the gap between the particle and the wall turns thin, the particle can even move faster than it would at $a/b = 0$. For example, as $C_t^* = 2C_m^* = 0.02$, $k^* = 100$, and $a/b = 0.99$, the thermophoretic velocity can be as much as 54% higher than the value with the wall being far away from the particle. This interesting feature that U/U_0 may not be a monotonic function of a/b and can even be greater than unity is understandable because the wall effect of hydrodynamic resistance on the particle is in competition with the wall effect of thermal enhancement when a particle with small $C_t^* = 2C_m^*$ and large k^* is undergoing thermophoretic motion normal to a plane wall. Under the situations of relatively small k^* (or relatively large C_t^* and C_m^*), the thermophoretic mobility of the particle near the wall is a monotonic decreasing function of a/b. By the linearity of the problem, the magnitude of the thermophoretic velocity is independent of whether the particle migrates toward or away from the plane wall.

Figure 3 shows the effect of variation in C_t^* ($= 2C_m^*$, proportional to the Knudsen number l/a) on the wall-corrected normalized thermophoretic velocity U/U_0 for the cases of $k^* = 100$ and 1. There exists a maximum along each curve for the velocity of a particle with large values of k^* and a/b. It is understandable that U/U_0 decreases with an increase in C_t^* but increases with the accompanying increase in C_m^*, and the competition between these two opposite effects leads to a maximum of U/U_0 (whose value can be greater than unity in case k^* is large). In general, these maximum points occur in the vicinity of $C_m^* = 0.01$.

The effect of varying the relative thermal conductivity k^* on the wall-corrected normalized particle velocity U/U_0 is illustrated in Figure 4 for the cases of $C_t^* = 2C_m^* = 0.02$ and 0.2. As expected, the curves for U/U_0 versus k^* show a monotonically increasing trend; if the values of k^* and a/b are sufficiently large, the value of U/U_0 can be greater than unity for the case of $C_t^* = 2C_m^* = 0.02$.

For the creeping motion of a spherical aerosol particle with a frictional (but isothermal) slip surface on which a constant body force $F\boldsymbol{e}_z$ (such as a gravitational field) is exerted normal to an infinite plane wall, the exact result of the particle velocity has recently been developed by using the boundary-collocation technique.[32] A comparison of the boundary effects on the motion of the aerosol sphere under gravity [in which $U_0 = (F/6\pi\eta_f a)(1 + 3C_m^*)/(1 + 2C_m^*)$] and on the thermophoresis is given in Figure 5. Obviously, the wall effect on thermophoretic motion is much weaker than that on a sedimenting particle. Note that the wall effect on the particle motion in a gravitational field is stronger when the value of C_m^* becomes smaller, which is different from what would occur if a particle with a relatively large value of C_m^* migrates near a plane wall due to a thermophoretic driving force.

Because the governing equations and boundary conditions concerning the general problem of thermophoresis of a particle in an arbitrary direction near a plane wall are linear, the net solution can be obtained as a superposition of the solutions for its two subproblems: motion perpendicular to the plane, which is examined in this article, and motion parallel to the plane. The collocation solutions for the thermophoretic motion of a spherical particle parallel to a plane wall have already been obtained by Keh and Chen.[26] It was found that, when the wall is prescribed with a linear temperature profile consistent with the

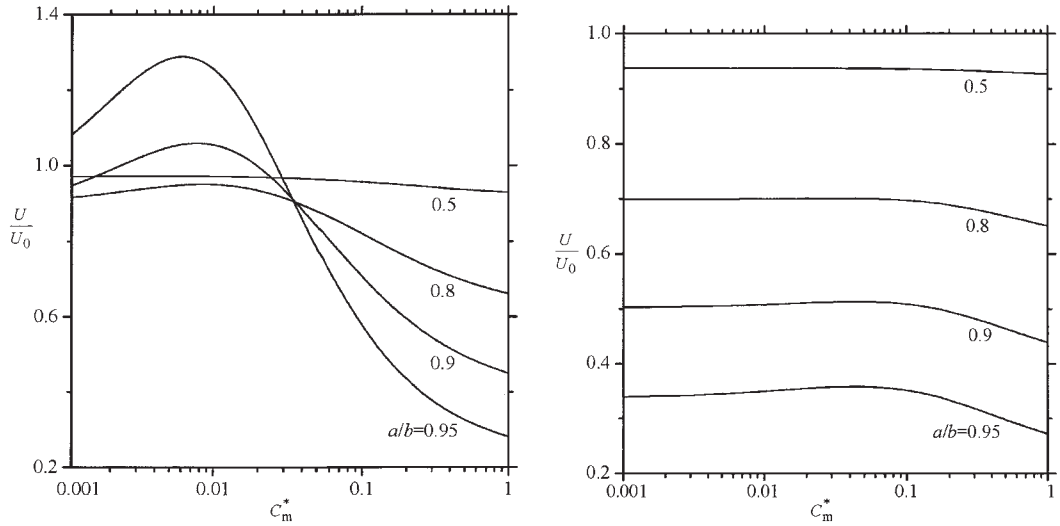

Figure 3. Plots of the normalized thermophoretic velocity U/U_0 of a spherical particle with $C_t^* = 2C_m^*$ perpendicular to a plane wall vs. the normalized frictional slip coefficient for various values of the separation parameter a/b.

(a) With $k^* = 100$; (b) with $k^* = 1$.

far-field temperature distribution, the wall-corrected normalized thermophoretic velocity of the particle also increases with an increase in k^*. A comparison between the Table 2 of Keh and Chen and our Table 1 indicates that the plane wall in general exerts the most influence on the particle when thermophoretic motion occurs normal to it, and the least in the case of thermophoresis parallel to it. Therefore, the direction of motion of a particle near a plane wall is different from that of the prescribed thermal gradient, except when it is oriented parallel or perpendicular to the plane wall.

Motion perpendicular to two plane walls

Numerical results of the normalized thermophoretic velocity U/U_0 of a spherical particle with $C_t^* = 2C_m^* = 0$ and 0.02 perpendicular to two parallel plane walls with equal distances from the particle ($c = b$) are presented in Table 2 for various values of the parameters k^* and a/b using the boundary collocation method. In the Appendix, an approximate analytical solution for the same thermophoretic motion as that considered here is also obtained by using the method of reflections. This solution is given by Eq. A13, which is a power series expansion in λ ($= a/b$). The values of the wall-corrected normalized particle velocity calculated from this asymptotic solution, with the $O(\lambda^9)$ term neglected, are also listed in Table 2 for comparison. Similar to the case of migration of a spherical particle normal to a single plane wall considered in the previous subsection, the approximate analytical formula of Eq. A13 agrees quite well with the exact results as long as $\lambda \leq 0.6$, but can

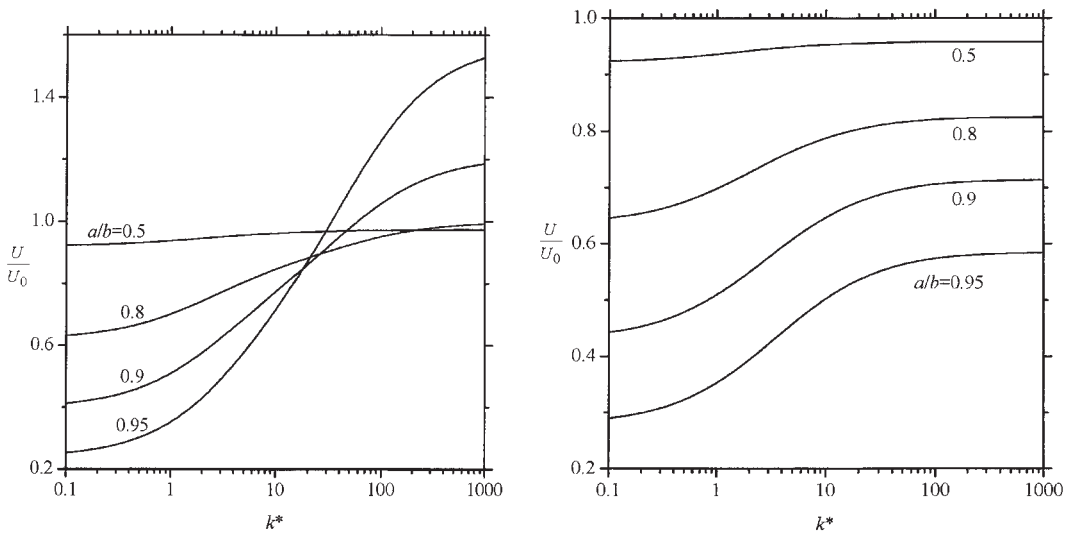

Figure 4. Plots of the normalized thermophoretic velocity U/U_0 of a spherical particle perpendicular to a plane wall vs. the relative thermal conductivity of the particle for various values of the separation parameter a/b.

(a) With $C_t^* = 2C_m^* = 0.02$; (b) with $C_t^* = 2C_m^* = 0.2$.

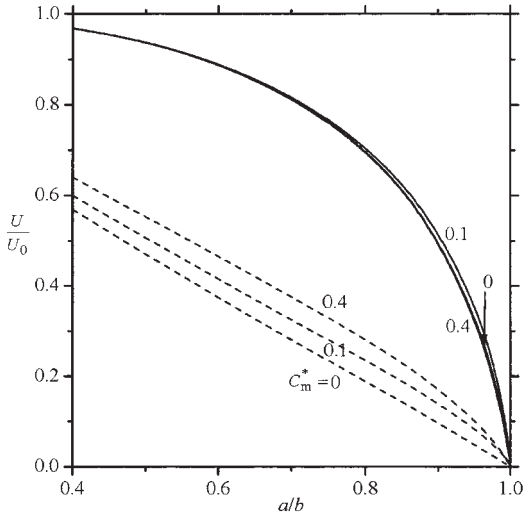

Figure 5. Plots of the normalized thermophoretic mobility (solid curves, with $C_t = 2C_m$ and $k^* = (1 - C_t^*)^{-1}$) and sedimenting mobility (dashed curves) of a spherical particle migrating perpendicular to a plane wall vs. the separation parameter *a/b* for different values of C_m^*.

have significant errors when $\lambda \geq 0.8$. Again, Eq. A13 can overestimate or underestimate the thermophoretic velocity of the particle. A comparison between Table 2 for the case of a slit and Table 1 for the case of a single normal plane indicates that the assumption that the boundary effect for two walls can be obtained by simple addition of single-wall effects may lead to a greater or smaller correction to thermophoretic motion.

The collocation results for the normalized thermophoretic mobility U/U_0 of a spherical particle with $C_t^* = 2C_m^* = 0.02$ and 0.2 located midway between two parallel plane walls (with $c = b$) caused by a perpendicular thermal gradient are plotted in Figure 6 as a function of a/b for various values of k^*. Analogous to the corresponding motion of a particle normal to a single plane wall, for specified values of C_t^*, C_m^*, and a/b, U/U_0 increases with an increase in k^*. Again, for a case shown in Figure 6a with some small values of C_t^* and C_m^* under the situation of large k^*, the thermophoretic mobility of the particle first goes through a minimum with the increase of a/b from $a/b = 0$ and then increases to a certain extent, and the particle can even move faster than it would at $a/b = 0$. This result indicates that the effect of thermal enhancement, rather than that of hydrodynamic resistance, can be overriding under some circumstances. An examination of the asymptotic formula for U/U_0 in Eq. A13 also shows a good agreement of the trend in Figure 6 with the analytical solution. For other cases, U/U_0 decreases monotonically with an increase in a/b.

A careful comparison of the curves in Figure 6a for the case of a slit with the corresponding curves in Figure 2a for the case of a single wall reveals an interesting feature of the boundary effect on thermophoresis of an aerosol sphere. The presence of a second, normal plane wall, even at a symmetric position with respect to the sphere against the first, does not always enhance the wall effect on the thermophoretic particle induced by the first plate only. This result reflects again the fact that the wall can affect the thermal driving force and the viscous drag force on a particle in opposite directions for some cases. Each force is increased in its own direction as the value of a/b turns small, but to a different degree, for the case of lateral thermophoretic motion of a particle in a slit relative to that for the case of migration normal to a single plate. Thus, the net effect composed of these two opposite forces for the slit case is not necessarily to enhance that for the case of a single wall.

In Figure 7a, the collocation results for the normalized velocity U/U_0 of an aerosol sphere with $k^* = (1 - C_t^*)^{-1}$ undergoing thermophoresis normal to two plane walls at various positions between them are plotted for the case of $C_t^* = 2C_m^* = 0.2$. The dashed curves (with a/b constant) illustrate the effect of the position of the second wall (at $z = c$) on the particle velocity for various values of the relative sphere-to-first-wall spacing b/a. The solid curves (with $2a/(b + c)$ constant) indicate the variation of the particle velocity as a function of the sphere position at various values of the relative wall-to-wall spacing $(b + c)/2a$. As illustrated in Figure 7a, the net wall effect is to reduce the thermophoretic mobility U/U_0 of the particle. At a constant value of $2a/(b + c)$, the particle experiences a minimum viscous drag force and has a greatest velocity when it is located midway between the two walls (with $c = b$). The hydrodynamic drag increases and the thermophoretic velocity decreases as the particle approaches either of

Table 2. Normalized Thermophoretic Velocity of a Spherical Particle Perpendicular to Two Equally Distant Plane Walls (with $c = b$) Computed from the Exact Boundary-Collocation Solution and the Asymptotic Method-of-Reflection Solution

	U/U_0			
	$C_t^* = 2C_m^* = 0$		$C_t^* = 2C_m^* = 0.02$	
a/b	Exact Solution	Asymptotic Solution	Exact Solution	Asymptotic Solution
		$k^* = 0$		
0.2	0.99143	0.99143	0.99142	0.99143
0.4	0.93503	0.93594	0.93498	0.93585
0.6	0.79470	0.81171	0.79474	0.81108
0.8	0.52842	0.64972	0.53111	0.64731
0.9	0.31579	0.58245	0.32454	0.57845
0.95	0.17547	0.55918	0.19034	0.55421
0.99	0.03872	0.54749	0.05597	0.54166
0.995	0.01963		0.03385	
0.999	0.00399		0.01012	
		$k^* = 10$		
0.2	0.99741	0.99741	0.99721	0.99722
0.4	0.98184	0.98227	0.98025	0.98061
0.6	0.94883	0.95711	0.94403	0.95086
0.8	0.90053	0.96391	0.89469	0.94570
0.9	0.87178	1.01727	0.87203	0.98717
0.95	0.85225	1.06977	0.85236	1.03119
0.99	0.76323	1.12967	0.66676	1.08265
0.995	0.68362		0.52471	
0.999	0.42811		0.21674	
		$k^* = 100$		
0.2	0.99847	0.99847	0.99820	0.99820
0.4	0.99056	0.99092	0.98864	0.98864
0.6	0.98147	0.98823	0.98070	0.97949
0.8	1.00817	1.05008	1.06470	1.02389
0.9	1.10667	1.15628	1.33315	1.11238
0.95	1.28728	1.24601	1.76367	1.18938
0.99	2.08026	1.34273	2.46653	1.27338
0.995	2.59557		2.25845	
0.999	4.05571		1.11697	

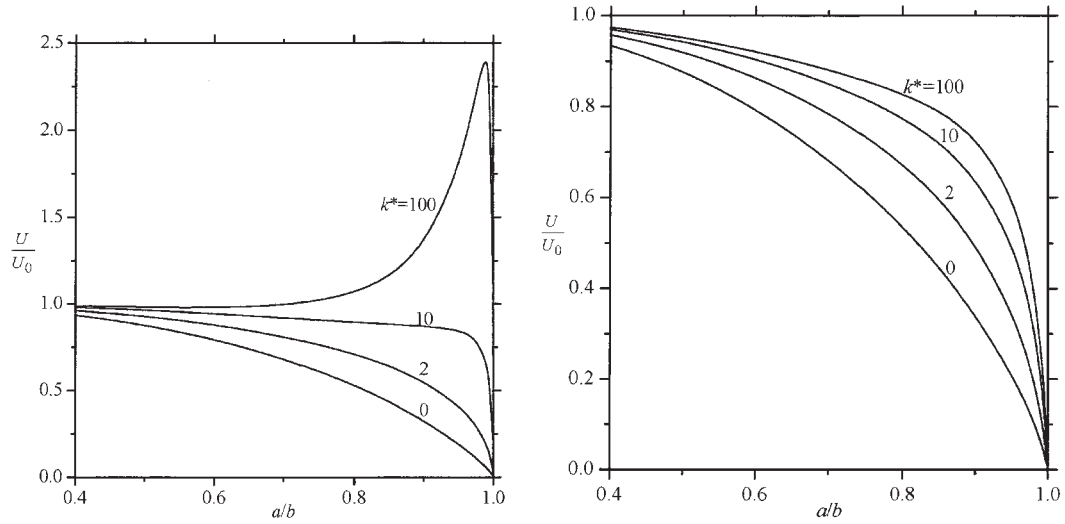

Figure 6. Plots of the normalized velocity U/U_0 of a spherical particle situated midway between two parallel plane walls (with c = b) undergoing thermophoresis perpendicularly versus the separation parameter a/b for various values of k^*.

(a) With $C_t^* = 2C_m^* = 0.02$; (b) with $C_t^* = 2C_m^* = 0.2$.

the walls (or the ratio $b/(b + c)$ decreases). Interestingly, at some specified values of a/b for the thermophoretic particle near a first wall, the presence of a second plate can increase the velocity of the particle when it is far from the particle (c is large), and then reduce the particle velocity when it is close to the particle (say, $b/(b + c) > 0.4$).

On the other hand, for some cases such as the migration of an aerosol sphere with a large value of k^* perpendicular to two plane walls as shown in Figures 7b and 8 ($k^* = 100$), the net wall effect can increase the thermophoretic mobility of the particle relative to its isolated value (when the values of C_t^* and C_m^* are small). At a fixed value of $2a/(b + c)$ in these cases, the normalized thermophoretic mobility of the particle has a relatively small value as it is located midway between the two walls, where the particle experiences a minimum effect of thermal enhancement, and becomes relatively large when it approaches either of the walls; the normalized particle mobility is not necessarily a monotonic function of $b/(b + c)$, the relative position of the particle between the two walls. Again, the effect of variation in C_t^* ($= 2C_m^*$) on the wall-corrected normalized particle velocity U/U_0 does not exhibit a monotonic trend.

The collocation solution for the problem of sedimentation of an aerosol sphere with a slip-flow surface perpendicular to two plane walls at an arbitrary position between them was also obtained.[32] Comparing that solution with the present results,

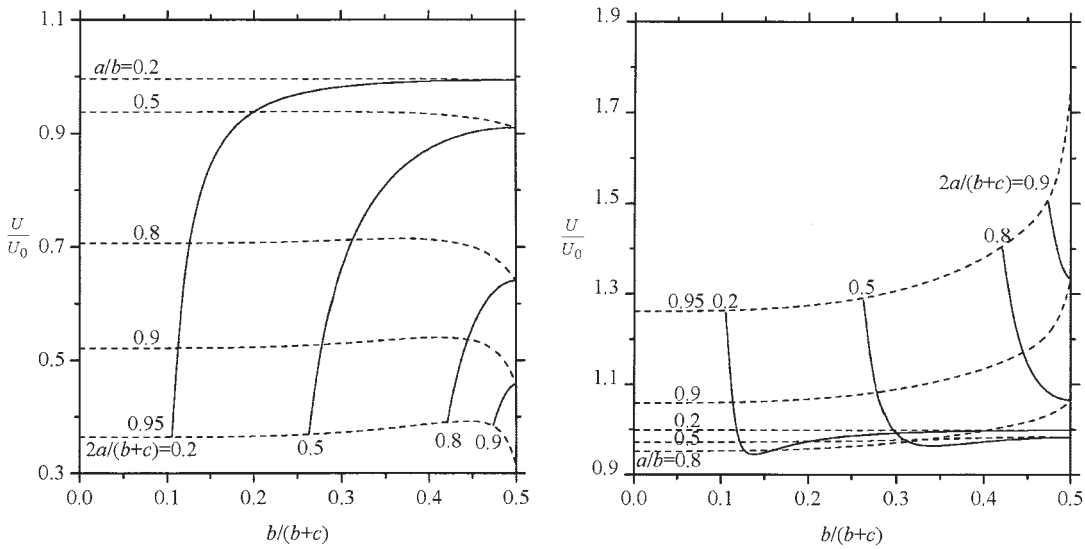

Figure 7. Plots of the normalized thermophoretic velocity U/U_0 of a spherical particle perpendicular to two plane walls vs. the ratio $b/(b + c)$ with a/b and $2a/(b + c)$ as parameters.

(a) With $k^* = (1 - C_t^*)^{-1}$ and $C_t^* = 2C_m^* = 0.2$; (b) with $k^* = 100$ and $C_t^* = 2C_m^* = 0.02$.

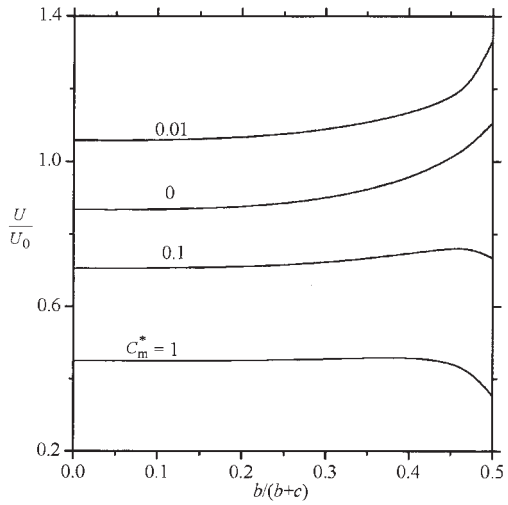

Figure 8. Plots of the normalized thermophoretic velocity U/U_0 of a spherical particle perpendicular to two plane walls vs. the ratio $b/(b + c)$ for the case of $C_t^* = 2C_m^*$, $k^* = 100$, and $a/b = 0.9$ with C_m^* as a parameter.

we still find that the wall effect on thermophoresis in general is much weaker than that on sedimentation.

Since the general problem of thermophoresis of a particle in an arbitrary direction between two parallel plane walls is linear, its solution can be obtained as the vectorial summation of the solutions for its two subproblems: motion perpendicular to the plane walls, which is examined in this paper, and motion parallel to the confining boundaries. The collocation solutions for the thermophoretic motion of a spherical particle parallel to two plane walls have already been obtained by Keh and Chen.[26] It was found that, when the walls are prescribed with a linear temperature profile consistent with the far-field temperature distribution, the wall-corrected normalized thermophoretic velocity of the particle also increases with an increase in k^*. A comparison between the Table 3 of Keh and Chen[26] and our Table 2 shows that the plane walls in general exert the most influence on the particle when thermophoretic motion occurs normal to them, and the least in the case of thermophoresis parallel to them. Therefore, the direction of thermophoretic motion of a particle between two parallel plane walls is different from that of the imposed thermal gradient, except when it is oriented parallel or perpendicular to the plane walls.

Concluding Remarks

The exact numerical solution and approximate analytical solution for the quasisteady thermophoretic motion of an aerosol sphere perpendicular to two infinite plane walls at an arbitrary position between them have been obtained in this work by using the boundary-collocation technique and the method of reflections, respectively, in the limit of vanishingly small Reynolds and Peclet numbers. It has been found that the boundary effect on thermophoretic motion of a particle is quite complicated. The thermophoretic mobility of a particle near a wall is generally, but not necessarily, a monotonic decreasing function of the separation parameter a/b. When the value of a/b is close to unity, the effect of a neighboring wall can speed up or slow down the particle velocity relative to its isolated value depending on the values of the parameters C_t^*, C_m^*, and k^* of the particle. This behavior reflects the competition between the weak hydrodynamic retardation exerted by the confining wall on the particle migration and the possible, relatively strong thermophoretic enhancement due to the thermal interaction between the particle and the wall. Unfortunately, no experimental data available in the literature involve the thermophoretic velocity of an aerosol particle as a function of its position between two parallel plane walls or near a single plane wall for a comparison with this theoretical prediction.

The thermophoretic mobility of a spherical particle parallel to two infinite plane walls at an arbitrary position between them was calculated in a previous work[26] for various values of the parameters C_t^* $(=2C_m^*)$, k^*, a/b, and $b/(b + c)$. It was also found that, for the case of the confining walls prescribed with the far-field temperature profile under the situation of large k^*, the particle mobility first decreases and then increases with increasing a/b. When the gaps between the particle and the plane walls turn thin, however, the particle can even migrate faster than it would when $a/b = 0$ (by as much as 21% for an example case of $C_t^* = 2C_m^* = 0$, $k^* = 10$, $c = b$, and $a/b = 0.99$), and the effect of viscous interactions is stronger or the effect of thermal interactions is weaker in a transverse thermophoresis than in a parallel motion. In general, the net boundary effect on thermophoresis of a particle is stronger for the perpendicular migration. For the general problem of a particle undergoing thermophoresis in an arbitrary direction with respect to the two parallel plane walls, the solution can be obtained by adding both the parallel and transverse results vectorially. These boundary effects should be considered when one estimates the thermophoretic deposition efficiency of aerosol particles in various applications, such as the scaling of heat transfer equipment or the removal of soot particles for combustion exhaust gas systems.

Throughout our analysis, fixed values of C_S, C_t, and C_m from the kinetic theory of gases are used everywhere along the particle surface. When the ratio a/b is close to unity, say, greater than 0.99, the gap region between the particle and the wall in which there is a fluid flow and the mean free path of the gas molecules is comparable in size. Perhaps the distributions of speeds and directions of the molecules bombarding the particle in the gap region differ from those in the bulk phase, leading to different values of C_S, C_t, and C_m there. However, this effect should be minor since the surface area percentage of the particle in the gap region is small.

It is worth repeating that our results are obtained on the basis of a continuum model for the gas phase with a slip-flow boundary condition at the particle surface. For a perfect gas, the kinetic theory predicts that the mean free path of gas molecules is inversely proportional to the pressure. As examples, the mean free path of air molecules at 25°C is about 67 nm at 1 atm and about 51 μm at 1 torr.[34] Therefore, our results obtained with the assumption of small Knudsen number can be used for a broad range of particle sizes (about 0.5 μm or larger) around atmospheric pressure but is only applicable for relatively large particles (about 0.1 mm or larger) at low pressures.

Acknowledgments

This research was partly supported by the National Science Council of the Republic of China.

Notation

a = radius of the particle, m
A = thermophoretic mobility defined by Eqs. 1 and 2, $m^2 \cdot s^{-1} \cdot K^{-1}$
$A(\omega)$, $B(\omega)$, $C(\omega)$, $D(\omega)$ = unknown functions in Eq. 21, $m^3 \cdot s^{-1}$
b, c = the respective distances from the particle center to the two plates, m
B = coefficients defined by Eq. 29e, $m^2 \cdot s^{-1} \cdot K^{-1}$
B_n, D_n = coefficients in Eqs. 22 and 23 for the flow field, $m^{n+2} \cdot s^{-1}$, $m^n \cdot s^{-1}$
C, D = dimensionless parameters defined by Eqs. 29a and 29b
C_m = dimensionless coefficient accounting for the frictional slip
C_m^* = $C_m l/a$
C_s = dimensionless coefficient accounting for the thermal slip
C_t = dimensionless coefficient accounting for the temperature jump
C_t^* = $C_t l/a$
$\mathbf{e}_z$, $\mathbf{e}_r$, $\mathbf{e}_\theta$ = unit vectors in z, r, and θ directions
E^2 = Stokes operator defined by Eq. 16, m^{-2}
E_∞ = $|\nabla T_\infty|$, $K \cdot m^{-1}$, $K \cdot m^{-1}$
G, H = dimensionless parameters defined by Eqs. 29c and 29d
$G_n^{-1/2}$ = Gegenbauer polynomial of the first kind of order n and degree $-1/2$
J_n = Bessel function of the first kind of order n
k = thermal conductivity of the fluid, $W \cdot m^{-1} \cdot K^{-1}$
k_1 = thermal conductivity of the particle, $W \cdot m^{-1} \cdot K^{-1}$
k^* = k_1/k
l = mean free path of the gas molecules, m
M, N = numbers of collocation points on the particle surface
P_n = Legendre function of order n
r = radial spherical coordinate, m
R_m, $\bar{R}_m$ = coefficients in Eqs. 10-12 for the temperature field, m^{m+2}, m^{-m+1}
T = temperature field in the fluid, K
T_1 = temperature field inside the particle, K
T_0 = mean fluid temperature in the vicinity of the particle, K
T_∞ = prescribed temperature field defined by Eq. 7, K
$\mathbf{U}$, U = particle velocity, $m \cdot s^{-1}$
$\mathbf{U}_0$, U_0 = velocity of an isolated particle, $m \cdot s^{-1}$
$\mathbf{v}$ = velocity field of the fluid, $m \cdot s^{-1}$
v_ρ, v_z = components of $\mathbf{v}$ in cylindrical coordinates, $m \cdot s^{-1}$
$X(w)$, $Y(w)$ = unknown functions in Eq. 9, m^3
z = axial cylindrical coordinate, m

Greek letters

$\gamma_{1n}^{(j)}$, $\gamma_{2n}^{(j)}$ = functions of r and θ defined by Eqs. B.4 and B.5, m^{-n-1}, m^{-n+1}
$\delta_m^{(1)}$, $\delta_m^{(2)}$, $\delta_m^{(3)}$ = functions of r and θ defined by Eqs. B1-B3, m^{-m-1}, m^{-m-2}, m^{-m-2}
η_f = viscosity of the fluid, $kg \cdot m^{-1} \cdot s^{-1}$
θ, ϕ = angular spherical coordinates
λ = a/b
ρ = radial cylindrical coordinate, m
ρ_f = density of the fluid, $kg \cdot m^{-3}$
Ψ = Stokes stream function for the external fluid flow, $m^3 \cdot s^{-1}$

Subscripts

p = particle
w = wall

Superscripts

(i) = the ith reflection

Literature Cited

1. Waldmann L, Schmitt KH. Thermophoresis and diffusiophoresis of aerosols. In: Davies CN *Aerosol Science.* New York: Academic Press; 1966:137-162.
2. Kennard EH. *Kinetic Theory of Gases.* New York: McGraw-Hill; 1938.
3. Friedlander SK. *Smoke, Dust and Haze.* New York: Wiley; 1977.
4. Sasse AGBM, Nazaroff WW, Gadgil AJ. Particle filter based on thermophoretic deposition from nature convection flow. *Aerosol Sci Technol.* 1994;20:227-238.
5. Montassier N, Boulaud D, Renoux A. Experimental study of thermophoretic particle deposition in laminar tube flow. *J Aerosol Sci.* 1991; 22:677-687.
6. Weinberg MC. Thermophoretic efficiency in modified chemical vapor deposition process. *J Am Ceram Soc.* 1982;65:81-87.
7. Ye Y, Pui DYH, Liu BYH, Opiolka S, Blumhorst S, Fissan H. Thermophoretic effect of particle deposition on a free standing semiconductor wafer in a clean room. *J Aerosol Sci.* 1991;22:63-72.
8. Williams MMR, Loyalka SK. *Aerosol Science*: *Theory and Practice, with Special Applications to the Nuclear Industry.* Oxford: Pergamon Press; 1991.
9. Messerer A, Niessner R, Poschl U. Thermophoretic deposition of soot aerosol particles under experimental conditions relevant for modern diesel engine exhaust gas systems. *J Aerosol Sci.* 2003;34:1009-1021.
10. Messerer A, Niessner R, Poschl U. Miniature pipe bundle heat exchanger for thermophoretic deposition of ultrafine soot aerosol particles at high flow velocities. *Aerosol Sci Technol.* 2004;38:456-466.
11. Brock JR. On the theory of thermal forces acting on aerosol particles. *J Colloid Sci.* 1962;17:768-780.
12. Talbot L, Cheng RK, Schefer RW, Willis DR. Thermophoresis of particles in heated boundary layer. *J Fluid Mech.* 1980;101:737-758.
13. Keh HJ, Yu JL. Migration of aerosol spheres under the combined action of thermophoretic and gravitational effects. *Aerosol Sci Technol.* 1995;22:250-260.
14. Keh HJ, Chen SH. Particle interactions in thermophoresis. *Chem Eng Sci.* 1995;50:3395-3407.
15. Schadt CF, Cadle RD. Thermal forces on aerosol particles. *J Phys Chem.* 1961;65:1689-1694.
16. Li W, Davis EJ. Measurement of the thermophoretic force by electrodynamic levitation: microspheres in air. *J Aerosol Sci.* 1995;26:1063-1083.
17. Derjaguin BV, Storozhilova AI, Rabinovich YaI. Experimental verification of the theory of thermophoresis of aerosol particles. *J Colloid Interface Sci.* 1966;21:35-58.
18. Derjaguin BV, Rabinovich YaI, Storozhilova AI, Shcherbina GI. Measurement of the coefficient of thermal slip of gases and the thermophoresis velocity of large-size aerosol particles. *J Colloid Interface Sci.* 1976;57:451-461.
19. Cercignani C. *Rarefied Gas Dynamics: From Basic Concepts to Actual Calculations.* Cambridge: Cambridge Univ. Press; 2000.
20. Sone Y. *Kinetic Theory and Fluid Dynamics.* Boston: Birkhauser; 2002.
21. Chen SH, Keh HJ. Axisymmetric thermophoretic motion of two spheres. *J Aerosol Sci.* 1995;26:429-444.
22. Chen SH. Boundary effects on a thermophoretic sphere in an arbitrary direction of a plane surface. *AIChE J.* 2000;46:2352-2368.
23. Keh HJ, Chang JH. Boundary effects on the creeping-flow and thermophoretic motions of an aerosol particle in a spherical cavity. *Chem Eng Sci.* 1998;53:2365-2377.
24. Lu SY, Lee CT. Thermophoretic motion of an aerosol particle in a non-concentric pore. *J Aerosol Sci.* 2001;32:1341-1358.
25. Lu SY, Lee CT. Thermophoretic motion of a spherical aerosol particle in a cylindrical pore. *Aerosol Sci Technol.* 2003;37:455-459.
26. Keh HJ, Chen PY. Thermophoresis of an aerosol sphere parallel to one or two plane walls. *AIChE J.* 2003;49:2283-2299.
27. Lienhard JH. *A Heat Transfer Textbook* (2nd ed.). Englewood Cliffs, NJ: Prentice-Hall; 1987.
28. O'Brien V. Form factors for deformed spheroids in Stokes flow. *AIChE J.* 1968;14:870-875.
29. Ganatos P, Weinbaum S, Pfeffer R. A strong interaction theory for the creeping motion of a sphere between plane parallel boundaries. Part 1. Perpendicular motion. *J Fluid Mech.* 1980;99:739-753.
30. Chen SH, Keh HJ. Axisymmetric motion of two spherical particles with slip surfaces. *J Colloid Interface Sci.* 1995;171:63-72.
31. Happel J, Brenner H. *Low Reynolds number Hydrodynamics.* Dordrecht, The Netherlands: Nijhoff; 1983.
32. Chang YC, Keh HJ. Slow motion of a slip spherical particle perpen-

dicular to two plane walls. *J Fluids Structures*. submitted for publication, 2006.
33. Keh HJ, Lien LC. Electrophoresis of a colloidal sphere along the axis of a circular orifice or a circular disk. *J Fluid Mech.* 1991;224:305-333.
34. Shoemaker DP, Garland CW, Steinfeld JI, Nibler JW. *Experiments in Physical Chemistry* (4th ed.). New York: McGraw-Hill; 1981.

Appendix

Analysis of the thermophoresis of a spherical particle perpendicular to two plane walls by a method of reflections

In this appendix, we analyze the quasisteady thermophoretic motion of an aerosol sphere with the relative thermal conductivity k^*, temperature jump coefficient C_t^*, and frictional slip coefficient C_m^* located at the median plane between two parallel plates ($c = b$) in the direction perpendicular to them, as shown in Figure 1, by a method of reflections. The effect of the walls on the thermophoretic velocity $\mathbf{U}$ of the particle is sought in an expansion, which equals a/b, of the ratio of the particle radius to the distance between each wall and the center of the particle.

For the problem of thermophoresis of a spherical particle perpendicular to two plane walls with equal distances from the particle under a uniform thermal gradient $-E_\infty \mathbf{e}_z$, the governing equations 3a and 14 must be solved by satisfying the boundary conditions 4-7 and 17-19 with $c = b$. The method-of-reflection solution consists of the following series, whose terms depend on increasing powers of λ:

$$T = T_0 - E_\infty z + T_p^{(1)} + T_w^{(1)} + T_p^{(2)} + T_w^{(2)} + \ldots, \quad \text{(A1a)}$$

$$\mathbf{v} = \mathbf{v}_p^{(1)} + \mathbf{v}_w^{(1)} + \mathbf{v}_p^{(2)} + \mathbf{v}_w^{(2)} + \ldots, \quad \text{(A1b)}$$

where subscripts w and p represent the reflections from the wall and particle, respectively, and the superscript (i) denotes the ith reflection from that surface. In these series, all the expansion sets of the corresponding temperature and velocity for the fluid phase must satisfy Eqs. 3a and 14. The advantage of this method is that it is necessary to consider boundary conditions associated with only one surface at a time.

According to Eq. A1, the velocity of the particle can also be expressed in the series form,

$$\mathbf{U} = U_0 \mathbf{e}_z + \mathbf{U}^{(1)} + \mathbf{U}^{(2)} + \ldots. \quad \text{(A2)}$$

In this expression, $U_0 = AE_\infty$ is the thermophoretic velocity of an identical particle suspended freely in the continuous phase far from the walls given by Eqs. 1 and 2; $\mathbf{U}^{(i)}$ is related to $\nabla T_w^{(i)}$ and $\mathbf{v}_w^{(i)}$ by[14]:

$$\mathbf{U}^{(i)} = -A[\nabla T_w^{(i)}]_0 + [\mathbf{v}_w^{(i)}]_0 + \frac{a^2 D}{6}[\nabla^2 \mathbf{v}_w^{(i)}]_0. \quad \text{(A3)}$$

Here, D is defined by Eq. 29a, and the subscript 0 to variables inside brackets denotes evaluation at the position of the particle center.

The solution for the first reflected field from the particle is

$$T_p^{(1)} = -GE_\infty a^3 r^{-2} \cos\theta, \quad \text{(A4a)}$$

$$\mathbf{v}_p^{(1)} = \frac{1}{2} U_0 a^3 r^{-3} (2\cos\theta \mathbf{e}_r + \sin\theta \mathbf{e}_\theta), \quad \text{(A4b)}$$

where G is defined by Eq. 29c. Obviously, $-1 \le G \le 1/2$, with the upper and lower bounds occurring at the limits $k^* = 0$ and $k^* \to \infty$ (when $C_t^* \ll 1$), respectively. The velocity distribution shown in Eq. A4b is identical to the irrotational flow surrounding a rigid sphere moving with velocity $U_0 \mathbf{e}_z$.

The boundary conditions for the ith reflected fields from the walls are derived from Eqs. 5-7, 18, and 19:

$$|z| = b: \quad T_w^{(i)} = -T_p^{(i)}, \quad \text{(A5a)}$$

$$\mathbf{v}_w^{(i)} = -\mathbf{v}_p^{(i)}; \quad \text{(A5b)}$$

$$\rho \to \infty: \quad T_w^{(i)} \to 0, \quad \text{(A5c)}$$

$$\mathbf{v}_w^{(i)} \to \mathbf{0}. \quad \text{(A5d)}$$

The solution of $T_w^{(1)}$ is obtained by applying Hankel transforms on the variable ρ in Eqs. 3a and A5a, c (taking $i = 1$), with the result

$$T_w^{(1)} = GE_\infty a \lambda^2 \int_0^\infty \frac{1 + e^{-2\alpha}}{\sinh(2\alpha)} \sinh\left(\frac{\alpha}{b} z\right) \alpha J_0\left(\frac{\alpha}{b} \rho\right) d\alpha. \quad \text{(A6a)}$$

The solution for $\mathbf{v}_w^{(1)}$ can also be found by applying Hankel transforms to the Stokes equation 14 twice and to the boundary conditions A5b, d, which results in

$$\mathbf{v}_w^{(1)} = -\frac{1}{2} U_0 \lambda^3 \int_0^\infty \alpha^2 \left[E(\alpha, z) J_1\left(\frac{\alpha}{b}\rho\right) \mathbf{e}_\rho + F(\alpha, z) J_0\left(\frac{\alpha}{b}\rho\right) \mathbf{e}_z \right] d\alpha, \quad \text{(A6b)}$$

where

$$E(\alpha, z) = \frac{2}{2\alpha + \sinh(2\alpha)} \left[(1 - \alpha - e^{-\alpha}\sinh\alpha) \sinh\left(\frac{\alpha}{b} z\right) + \frac{\alpha}{b} z \cosh\left(\frac{\alpha}{b} z\right) \right], \quad \text{(A7a)}$$

$$F(\alpha, z) = \frac{2}{2\alpha + \sinh(2\alpha)} \left[(\alpha + e^{-\alpha}\sinh\alpha) \cosh\left(\frac{\alpha}{b} z\right) - \frac{\alpha}{b} z \sinh\left(\frac{\alpha}{b} z\right) \right]. \quad \text{(A7b)}$$

The contributions of $F_w^{(1)}$ and $\mathbf{v}_w^{(1)}$ to the velocity of the particle are determined by using Eq. A3:

$$\mathbf{U}_{\mathrm{t}}^{(1)} = -A[\nabla T_{\mathrm{w}}^{(1)}]_{r=0} = -d_1 G\lambda^3 U_0 \mathbf{e}_z, \tag{A8a}$$

$$\mathbf{U}_{\mathrm{h}}^{(1)} = \left[\mathbf{v}_{\mathrm{w}}^{(1)} + \frac{a^2}{6} D\nabla^2 \mathbf{v}_{\mathrm{w}}^{(1)}\right]_{r=0} = [-d_2\lambda^3 + d_3 D\lambda^5] U_0 \mathbf{e}_z, \tag{A8b}$$

$$\mathbf{U}^{(1)} = \mathbf{U}_{\mathrm{t}}^{(1)} + \mathbf{U}_{\mathrm{h}}^{(1)} = [-(d_2 + d_1 G)\lambda^3 + d_3 D\lambda^5] U_0 \mathbf{e}_z, \tag{A8c}$$

where

$$d_1 = \int_0^\infty \frac{1 + e^{-2\alpha}}{\sinh(2\alpha)} \alpha^2 \mathrm{d}\alpha = 0.60103, \tag{A9a}$$

$$d_2 = \int_0^\infty \frac{\sinh(\alpha) e^{-\alpha} + \alpha}{2\alpha + \sinh(2\alpha)} \alpha^2 \mathrm{d}\alpha = 0.79076, \tag{A9b}$$

$$d_3 = \frac{1}{3} \int_0^\infty \frac{\alpha^4}{2\alpha + \sinh(2\alpha)} \mathrm{d}\alpha = 0.44175. \tag{A9c}$$

Equation A8a shows that the reflected temperature field from the plane walls can decrease (if $G > 0$ or $k^* < (1 - C_{\mathrm{t}}^*)^{-1}$) or increase (if $G < 0$ or $k^* > (1 - C_{\mathrm{t}}^*)^{-1}$) the thermophoretic velocity of the particle, while Eq. A8b indicates that the reflected velocity field is to decrease this velocity; the net effect of the reflected fields is expressed by Eq. A8c, which can enhance or retard the movement of the particle, depending on the combination of the values of G (or k^* and C_{t}^*), D (or C_{m}^*), and λ. When $G = 0$ (or $k^* = (1 - C_{\mathrm{t}}^*)^{-1}$), the reflected temperature field makes no contribution to the thermophoretic velocity. Equation A8c indicates that the wall correction to the thermophoretic velocity of the particle is $\mathrm{O}(\lambda^3)$, which is weaker than that obtained for the corresponding sedimentation problem, in which the leading boundary effect is $\mathrm{O}(\lambda)$. Note that, when the values of C_{t}^* and C_{m}^* are small, the necessary condition for the wall enhancement on the thermophoretic motion to occur is a large value of k^* and a value of λ close to unity such that the relation $d_3 D\lambda^5 > (d_2 + d_1 G)\lambda^3$ is warranted.

The solution for the second reflected field from the particle is

$$T_{\mathrm{p}}^{(2)} = E_\infty [d_1 G^2 \lambda^3 a^3 r^{-2} \cos\theta + \mathrm{O}(\lambda^5 a^5)], \tag{A10a}$$

$$\mathbf{v}_{\mathrm{p}}^{(2)} = -\frac{1}{2} U_0 d_1 G\lambda^3 a^3 r^{-3} (2\cos\theta \mathbf{e}_r + \sin\theta \mathbf{e}_\theta) + O(\lambda^5 a^3). \tag{A10b}$$

The boundary conditions for the second reflected field from the walls are obtained by substituting the results of $T_{\mathrm{p}}^{(2)}$ and $\mathbf{v}_{\mathrm{p}}^{(2)}$ into Eq. A5, with which Eqs. 3a and 14 can be solved as before to yield

$$[\nabla T_{\mathrm{w}}^{(2)}]_{r=0} = -E_\infty [d_1^2 G^2 \lambda^6 + O(\lambda^9)] \mathbf{e}_z, \tag{A11a}$$

$$\left[\nabla \mathbf{v}_{\mathrm{w}}^{(2)} + \frac{a^2}{6} D\nabla^2 \mathbf{v}_{\mathrm{w}}^{(2)}\right]_{r=0} = U_0 [d_1 d_2 G\lambda^6 - d_1 d_3 DG\lambda^8 + O(\lambda^9)] \mathbf{e}_z. \tag{A11b}$$

The contribution of the second reflected field to the velocity of the particle is obtained by combining Eqs. A3 and A11, which gives

$$\mathbf{U}^{(2)} = [(d_1^2 G^2 + d_1 d_2 G)\lambda^6 - d_1 d_3 DG\lambda^8 + O(\lambda^9)] U_0 \mathbf{e}_z. \tag{A12}$$

Obviously, $\mathbf{U}^{(3)}$ will be $\mathrm{O}(\lambda^9)$. With the substitution of Eqs. A8c and A12 into Eq. A2, the particle velocity can be expressed as $\mathbf{U} = U\mathbf{e}_z$ with

$$U = U_0 [1 - (d_2 + d_1 G)\lambda^3 + d_3 D\lambda^5 + (d_1^2 G^2 + d_1 d_2 G)\lambda^6 - d_1 d_3 DG\lambda^8 + O(\lambda^9)]. \tag{A13}$$

This result is valid for a particle undergoing thermophoresis toward either of the two plane walls.

Definitions of some functions in the second section

The functions $\delta_m^{(j)}$ for j equal to 1, 2, or 3 in Eqs. 12, 13, and 24 are defined by

$$\delta_m^{(1)}(r, \theta) = \int_0^\infty \omega(\sinh^{-1}\tau)[-B'_{1m}(\omega, -b)\sinh\eta + B''_{1m}(\omega, c)\sinh\sigma] J_0(\omega r \sin\theta)\mathrm{d}\omega + r^{-m-1} P_m(\cos\theta), \tag{B1}$$

$$\delta_m^{(2)}(r, \theta) = \int_0^\infty \omega^2(\sinh^{-1}\tau)\{\sin\theta[B''_{1m}(\omega, -b)\sinh\eta - B''_{1m}(\omega, c)\sinh\sigma] J_1(r\omega\sin\theta) + \cos\theta[-B'_{1m}(\omega, -b)\cosh\eta + B''_{1m}(\omega, c)\cosh\sigma] J_0(r\omega\sin\theta)\}\mathrm{d}\omega - (m+1) r^{-m-2} P_m(\cos\theta), \tag{B2}$$

$$\delta_m^{(3)}(r, \theta) = \int_0^\infty \omega^2(\sinh^{-1}\tau)\{\cos\theta[B''_{1m}(\omega, -b)\sinh\eta - B''_{1m}(\omega, c)\sinh\sigma] J_1(r\omega\sin\theta) + \sin\theta[B''_{1m}(\omega, -b)\cosh\eta - B''_{1m}(\omega, c)\cosh\sigma] J_0(r\omega\sin\theta)\}\mathrm{d}\omega + mr^{-m-2}[P_m(\cos\theta)\cos\theta - P_{m-1}(\cos\theta)]\csc\theta; \tag{B3}$$

and the functions $\gamma_{in}^{(j)}$ for i and j equal to 1 or 2 in Eqs. 23 and 24 are defined by

$$\gamma_{in}^{(1)}(r, \theta) = -\int_0^\infty [G''_+(\sigma, \eta) B'_{in}(\omega, -b) - G''_+(\eta, \sigma) B'_{in}(\omega, c) - G'_+(\sigma, \eta) B''_{in}(\omega, -b) + G'_+(\eta, \sigma) B''_{in}(\omega, c)]\omega J_1(\omega r \sin\theta)\mathrm{d}\omega$$

$$- r^{-n+2i-3}[(n+1)G_{n+1}^{-1/2}(\cos\theta)\csc\theta - 2(i-1)G_n^{-1/2}(\cos\theta)\cot\theta], \quad \text{(B4)}$$

$$\gamma_{in}^{(2)}(r,\theta) = -\int_0^\infty [-G'_-(\sigma,\eta)B'_{in}(\omega,-b) + G'_-(\eta,\sigma)B'_{in}(\omega,c) + G''_-(\sigma,\eta)B''_{in}(\omega,-b) - G''_-(\eta,\sigma)B''_{in}(\omega,c)]\omega J_0(\omega r\sin\theta)\mathrm{d}\omega - r^{-n+2i-3}[P_n(\cos\theta) + 2(i-1)G_n^{-1/2}(\cos\theta)], \quad \text{(B5)}$$

where

$$B'_{1n}(\omega,z) = -\frac{1}{n!}\left(\frac{\omega|z|}{z}\right)^{n-1}e^{-\omega|z|}, \quad \text{(B6)}$$

$$B''_{1n}(\omega,z) = -\frac{\omega^{n-1}}{n!}\left(\frac{|z|}{z}\right)^{n}e^{-\omega|z|}, \quad \text{(B7)}$$

$$B'_{2n}(\omega,z) = -\frac{1}{n!}\left(\frac{\omega|z|}{z}\right)^{n-3}[(2n-3)\omega|z| - n(n-2)]e^{-\omega|z|}, \quad \text{(B8)}$$

$$B''_{2n}(\omega,z) = -\frac{\omega^{n-3}}{n!}\left(\frac{|z|}{z}\right)^{n}[(2n-3)\omega|z| - (n-1)(n-3)]e^{-\omega|z|}; \quad \text{(B9)}$$

$$G'_\pm(\mu,\nu) = \tau^*\mu\nu(\mu' \pm \tau'\nu'), \quad \text{(B10)}$$

$$G''_\pm(\mu,\nu) = \tau^*[\nu(\cosh\mu - \tau'\nu') \pm \mu(\mu' - \tau'\cosh\nu)]; \quad \text{(B11)}$$

$$\mu' = \frac{\sinh\mu}{\mu}, \quad \nu' = \frac{\sinh\nu}{\nu}, \quad \tau' = \frac{\sinh\tau}{\tau}, \quad \tau^* = \frac{\tau}{\sinh^2\tau - \tau^2}, \quad \text{(B12)}$$

$$\sigma = \omega(r\cos\theta + b), \quad \eta = \omega(r\cos\theta - c), \quad \tau = \omega(b+c). \quad \text{(B13)}$$

The functions γ_{in}^* for i equal to 1 or 2 in Eq. 24 are defined by

$$\gamma_{in}^*(r,\theta) = -\cos\theta\sin\theta[C_{in}^*(r,\theta) + D_{in}^*(r,\theta)] - (\cos^2\theta - \sin^2\theta)[C_{in}^{**}(r,\theta) + D_{in}^{**}(r,\theta)], \quad \text{(B14)}$$

where

$$C_{1n}^*(r,\theta) = -2r^{-(n+2)}[(n+1)(n+\csc^2\theta)G_{n+1}^{-1/2}(\cos\theta) - (3n+2)P_n(\cos\theta)\cos\theta + nP_{n-1}(\cos\theta)], \quad \text{(B15)}$$

$$C_{2n}^*(r,\theta) = 2r^{-n}[2(2n-1+\cot^2\theta)G_n^{-1/2}(\cos\theta)\cos\theta - (n+1)(n-1+\cot^2\theta)G_{n+1}^{-1/2}(\cos\theta) - (n+2 - 4\sin^2\theta)P_{n-1}(\cos\theta) + 3nP_n(\cos\theta)\cos\theta], \quad \text{(B16)}$$

$$C_{1n}^{**}(r,\theta) = -r^{-(n+2)}\{n\cot\theta[(n+1)G_{n+1}^{-1/2}(\cos\theta) + P_{n-1}(\cos\theta)] + [(3n+2)\sin\theta - n\csc\theta]P_n(\cos\theta)\}, \quad \text{(B17)}$$

$$C_{2n}^{**}(r,\theta) = -r^{-n}\{2[2(n-1)\sin\theta - (n-2)\csc\theta]G_n^{-1/2}(\cos\theta) + (n^2-n-2)G_{n+1}^{-1/2}(\cos\theta)\cot\theta + (n-4\sin^2\theta)P_{n-1}(\cos\theta)\cot\theta + n(3\sin\theta - \csc\theta)P_n(\cos\theta)\}; \quad \text{(B18)}$$

$$D_{in}^*(r,\theta) = \int_0^\infty \{[G''_+(\sigma,\eta)B'_{in}(\omega,-b) - G''_+(\eta,\sigma)B'_{in}(\omega,c) - G'_+(\sigma,\eta)B''_{in}(\omega,-b) + G'_+(\eta,\sigma)B''_{in}(\omega,c)][J_0(\omega r\sin\theta) - J_2(\omega r\sin\theta)] + 2[G_-^*(\sigma,\eta)B'_{in}(\omega,-b) - G_-^*(\eta,\sigma)B'_{in}(\omega,c) - G_-^{**}(\sigma,\eta)B''_{in}(\omega,-b) + G_-^{**}(\eta,\sigma)B''_{in}(\omega,c)]J_0(\omega r\sin\theta)\}\omega^2\mathrm{d}\omega, \quad \text{(B19)}$$

$$D_{in}^{**}(r,\theta) = \int_0^\infty \{[G_+^{**}(\sigma,\eta)B'_{in}(\omega,-b) - G_+^{**}(\eta,\sigma)B'_{in}(\omega,c) - G_+^*(\sigma,\eta)B''_{in}(\omega,-b) + G_+^*(\eta,\sigma)B''_{in}(\omega,c)] + [G'_-(\sigma,\eta)B'_{in}(\omega,-b) - G'_-(\eta,\sigma)B'_{in}(\omega,c) - G''_-(\sigma,\eta)B''_{in}(\omega,-b) + G''_-(\eta,\sigma)B''_{in}(\omega,c)]\}\omega^2J_1(\omega r\sin\theta)\mathrm{d}\omega; \quad \text{(B20)}$$

and

$$G_\pm^*(\mu,\nu) = \tau^*[(\mu+\nu)(\mu' \pm \tau'\nu') + \nu(\cosh\mu - \mu') \pm \tau'\mu(\cosh\nu - \nu')], \quad \text{(B21)}$$

$$G_\pm^{**}(\mu,\nu) = \tau^*[\cosh\mu - \tau'\nu' \pm (\mu' - \tau'\cosh\nu) + \nu\sinh\mu - \tau'(\cosh\nu - \nu') \pm (\cosh\mu - \mu' - \tau'\mu\sinh\nu)]. \quad \text{(B22)}$$

Manuscript received Sept. 29, 2005, and revision received Jan. 4, 2006.